Published in final edited form as:
J Med Chem. 2011 July 14; 54(13): 4923–4927. doi:10.1021/jm200304y.

Synthesis and Evaluation of Diaryl Thiazole Derivatives that Inhibit Activation of Sterol Regulatory Element-Binding Proteins

Shinji Kamisuki[†], **Takashi Shirakawa**[†], **Akira Kugimiya**[†], **Lutfi Abu-Elheiga**[‡], **Hea-Young Park Choo**[†,§], **Kouhei Yamada**[†], **Hiroki Shimogawa**[†], **Salih J. Wakil**[*,‡], and **Motonari Uesugi**[*,†,‡]

[†] Institute for Chemical Research and Institute for Integrated Cell-Material Sciences, Kyoto University, Uji, Kyoto 611-0011, Japan

[‡] The Verna and Marrs McLean Department of Biochemistry and Molecular Biology, Baylor College of Medicine, Houston, TX 77030, U.S.A

Abstract

Fatostatin, a recently discovered small molecule that inhibits activation of sterol regulatory element-binding protein (SREBP), blocks biosynthesis and accumulation of fat in obese mice. The present study synthesized and evaluated a series of fatostatin derivatives. Our structure-activity relationships led to the identification of *N*-(4-(2-(2-propylpyridin-4-yl)thiazol-4-yl)phenyl)methanesulfonamide (**24**; FGH10019) as the most potent drug-like molecule among the analogs tested. Compound **24** has high aqueous solubility and membrane permeability, and may serve as a seed molecule for further development.

Introduction

Long-chain fatty acids are major sources of energy and important components of the lipids that compose cellular membranes. *De novo* lipid synthesis is activated in some types of cancers, and synthesized lipids are accumulated in the body in metabolic syndrome. Therefore, pharmacological intervention for *de novo* lipid synthesis may prove to be effective against a number of human diseases. The conversion of carbohydrates into lipids through *de novo* fatty acid involves at least twelve enzymatic reactions, and conversion through cholesterol synthesis involves at least twenty-three. Expression levels of the genes encoding these enzymes are controlled by transcription factors, which are designated sterol regulatory element-binding proteins (SREBPs).[1, 2] SREBPs are synthesized as ER membrane-bound precursors, and must be proteolytically released by two proteases bound to the Golgi membrane – Site-1 (S1P) and Site-2 (S2P) proteases – to generate forms that activate transcription of target genes in the nucleus.[1, 3] Activation of SREBPs is tightly regulated by negative feedback: sterols interact with SREBP cleavage-activating protein (SCAP), an ER membrane-bound escort protein of SREBPs, thereby retaining the SCAP/SREBP complex in the ER.[4, 5] Binding of the sterol to SCAP promotes the interaction of SCAP with INSIG, a retention protein in the ER.[6, 7] Thus, SREBPs are key lipogenic

[*]To whom correspondence should be addressed: uesugi@scl.kyoto-u.ac.jp (M.U.); swakil@bcm.edu (S.J.W.).
[§]Current address: Ewha Woman's University, Seoul 120-750, Korea

Conflict of interest statement: L.A.E., S.J.W., and M.U. have signed a scientific advisory agreement with a company founded to develop the technology described in this article.

Supporting Information Available: Supplementary data, synthesis of compounds **4-8**, **10**, **12**, **15-18**, **21-23**, **25**, and **26**, supplementary biological assay methods. This material is available free of charge via the Internet at http://pubs.acs.org.

transcription factors that govern the homeostasis of fat metabolism, and SCAP plays a pivotal role in the regulation of SREBPs.

We previously described a synthetic diaryl thiazole molecule, fatostatin (molecule **1**, Figure 1), and identified its target. Fatostatin (125B11) was originally discovered from a chemical library as a synthetic small molecule that inhibited insulin-induced adipogenesis and serum-independent growth of cancer cells in cell culture.[8] The molecule was later shown to selectively reduce the expression of SREBP target genes by blocking the activation of SREBP transcription factors.[9] The direct target of fatostatin appears to be SCAP; however, fatostatin does not affect the interaction of SCAP with SREBP-2 or insulin-induced gene (INSIG), and binds to SCAP at a site distinct from that of sterols.[9] Thus, fatostatin is a unique small molecule that blocks the activation of SREBPs independently of INSIG and sterols. Fatostatin or its analogs may serve as research tools for investigating the SREBP/SCAP pathway.

The structure of fatostatin also provides a model that may help direct the design of molecules for pharmacological intervention against cancer progression and metabolic diseases, including fatty liver disease. In fact, fatostatin downregulated the expression of lipogenic enzymes and blocked increases in body weight, blood glucose, and hepatic fat accumulation in obese *ob/ob* mice, even under uncontrolled food intake.[9] However, fatostatin showed only moderate potency in mice, and its utility was limited by low aqueous solubility. The present study synthesized a number of fatostatin derivatives and compared their potency and physicochemical properties, with the goal of identifying an analog with improved characteristics for use in further *in vivo* evaluation in a variety of disease models.

Chemistry

Fatostatin is composed of three aromatic rings: pyridine, thiazole and toluene. Four routes were used to synthesize fatostatin derivatives (Schemes 1–4). In the first route, a central thiazole ring was constructed by reacting various thioamide derivatives with α-bromoketone derivatives (Scheme 1). Thioamide **2** or **3** was coupled with an α-bromoketone precursor in warm ethanol to yield 4-phenyl-2-(pyridin-4-yl)thiazole derivatives (analogs **4**–**9**). The products crystallized directly from the reaction mixtures were filtered to provide high yields of pure thiazoles. Analog **10** was synthesized by the reaction of **3** with 2-bromo-1-(thiophen-2- yl)ethanone. Diphenyl thiazole **12** was similarly synthesized from benzothioamide (**11**) and 2-bromo-1- *p*-tolylethanone.

To prepare analog **15**, 4- bromo-2-propylpridine (**14**) was first synthesized from 4-bromopyridine (**13**), as previously described.[10] Suzuki coupling of bromide **14** with 4′-methyl-4- biphenylboronic acid produced analog **15** (Scheme 2).

Phenol derivatives (Scheme 3) were prepared by alkaline hydrolysis of analog **6**, producing the *p*-phenol derivative **16**, or demethylation of methyl ether **8** and **9** by BBr_3, producing the *m*-phenol derivative **17** and *o*-phenol derivative **18**.

Amine, amide, and sulfonamide derivatives were also synthesized (Scheme 4). Isopropyl amine **20**, benzyl amine **21**, and cyclopropylmethyl amine **22** were prepared in high yields by a direct reductive amination reaction of acetone, benzaldehyde, or cyclopropanecarboxaldehyde with a previously prepared primary amine **19**.[11] Amine **19** was also reacted with acetyl chloride, methane sulfonylchloride, thiophene sulfonylchloride, or tosyl chloride in the presence of pyridine to yield acetoamide **23**, methane sulfoneamide **24**, thiophene sulfoneamide **25**, and toluene sulfoneamide **26**, respectively.

Results and Discussion

All of the synthesized fatostatin derivatives were assayed for their ability to inhibit the expression of a luciferase reporter gene, in which expression of luciferase was controlled by three repeats of sterol regulatory elements (SREs). This SREBP-responsive reporter construct was co-transfected into Chinese hamster ovary-K1 (CHOK1) cells with a control β-gal reporter gene in which the expression of β-gal was driven by a constitutively active actin promoter. Luciferase expression from the SREBP-responsive reporter gene, normalized to β-gal expression, was activated upon lipid depletion.[9] Fatostatin decreased activation of the reporter gene with an IC_{50} value of 5.6 μM (Figure 2), which is consistent with results of previous studies.[9]

Replacement of any one of fatostatin's three aromatic rings with simpler aromatic structures affected activity. For example, analog **10**, a thiophene substitution, had an IC_{50} value of 14.7 μM in the reporter assay (Figure 2). Replacement of the 2-propylpridine group with phenyl group (analog **12**) resulted in a 3.3-fold decrease in potency. Analog **15**, which lacked the central thiazole of fatostatin, showed a large loss of activity, suggesting that the central thiazole moiety is important.

Changing the length of the alkyl chain at the 2-position of pyridine moiety also influenced activity of the fatostatin derivatives. Activity of the ethyl derivative (analog **4a**) was almost the same as that of fatostatin (Table 1). However, removal of *n*-propyl group (analog **4b**) resulted in reduced activity, suggesting that a lipophilic alkyl group at this position is essential.

The methyl group of toluene is often oxidized *in vivo* by cytochrome P450. Therefore, the effects of substitutions of the toluene moiety of fatostatin were examined (analogs **5**- **9** and **16**–**18**). Removal of the methyl group in the toluene moiety (analog **5a**) led to a fourfold decrease in potency (Table 2). Halogen substitutions (analogs **5b-d**), which are likely to be more metabolically stable than fatostatin, showed moderate activity. Incorporation of a large benzoyl group (analog **6**) resulted in potency similar to that of the halogenated derivatives. Hydrophilic substitutions, such as hydroxy and methoxy groups (analogs **7** and **16**) also failed to increase activity.

Effects of substitution at 2- and 3- positions of the benzene ring were examined, as well. 3-Methoxy, 3-hydroxy, and 2-hydroxy derivatives (analogs **8**, **17**, and **18**) were less potent than fatostatin. However, the 2-methoxy derivative (analog **9**) exhibited a slight increase in activity (Table 2), suggesting that substitution of the toluene moiety of fatostatin might further optimize potency and aqueous solubility. Therefore, further efforts were focused on substitution at the 4- position of the toluene moiety.

A variety of basic amine groups were introduced in the 4-position of the toluene moiety. The potency of an aniline derivative (analog **19**) was similar to that of fatostatin, and secondary amine derivatives (analogs **20**–**22**) showed slight improvement in activity (Table 3). Introduction of amide (analog **23**) or carbamate (analog **27**)[9] did not significantly improve potency; however, addition of sulfonamide (analogs **24**–**26**) increased activity. Analog **24**, with methanesulfonamide, exhibited the most potent activity: an IC_{50} value of 0.7 μM, comparable to the potency of an endogenous inhibitor, 25- hydroxycholesterol, which had an IC_{50} value of 0.3 μM.[12]

The inhibition of SREBP activation mediated by analog **24** was confirmed by Western blot analysis of SREBP-2 (Figure 3). Treatment of the CHO-K1 cells with analog **24** decreased the percentage of the mature form of SREBP-2 (68 kDa) at lower concentrations than treatment with fatostatin. Densitometric analysis of the gels indicated that the IC_{50} of analog

24 was approximately 1 μM, which is 5–10 times lower than the IC_{50} of fatostatin (~10 μM). The IC_{50} values were consistent with the values obtained via the reporter gene assays.

Fatostatin selectively downregulates endogenous SREBP-responsive genes in cultured human prostate cancer cells.[9] Real-time RT-PCR analysis of nine representative SREBPresponsive genes[13] was carried out to determine the selectivity of analog **24**. Transcription of all nine genes was downregulated by at least 25% (Figure 4). In contrast, treatment with analog **24** had no significant effect on transcription of three control genes unrelated to SREBP. Thus, the mode of action of analog **24** appears to be similar to that of fatostatin.

The *in silico* properties calculated for fatostatin and analogs **20** and **24** suggested that analog **24** has potential for further pharmaceutical development (see Supporting Information, Table S1). Typically, compounds that violate one or more of the "rule-of-five" – molecular weight >500 Da, logP >5, more than 5 H-bond donors, and more than 10 H-bond acceptors – are poorly absorbed.[14] Fatostatin and analog **20** violated one "rule-of-five"; their clogP values were 5.72 and 5.82, respectively. Analog **24** had a clogP value of 3.97, and a polar surface area of 108.57 $Å^2$. As expected, the *in vitro* aqueous solubility of analog **24** at pH 7 was more than 10 times higher than that of fatostatin or analog **20** (Table 4).

We examined other physicochemical properties of fatostatin and analogs **20** and **24**. The intrinsic clearance rates measured in mouse hepatocytes were 606, 272, and 137 ml min^{-1} kg^{-1}, respectively, and the corresponding half-lives ($t^{1/2}$) were 10.1, 22.4 and 44.4 min. Although fatostatin and analog **20** showed low metabolic stability in mouse hepatocytes, analog **24** was moderately stable.

Results of parallel artificial membrane permeability assays (PAMPA) indicated that passive permeability through an artificial membrane was low for fatostatin, moderate for analog **20**, and high for analog **24** (Table 5). Thus, analog **24** is likely to be have greater permeability *in vivo* than fatostatin or analog **20**. Warfarin (10 μM) was used as a control for the integrity of membrane. Retention of all compounds within the membrane was greater than 90%, probably due to the high lipophilicity of the compounds.

We previously demonstrated that intraperitoneal injection of fatostatin blocked increases in body weight, blood glucose and hepatic fat accumulation in obese *ob/ob* mice, even under conditions of uncontrolled food intake.[9] However, fatostatin was not suited for oral administration and further animal studies. To demonstrate oral availability of analog **24**, we provided *ob/ob* mice with ad libitum access over an 8-wk period to normal chow that contained analog **24**. The analog **24**-treated chow was fed at a dose rate calculated to provide about 0.7 mg analog **24** per day, at about 23 mg/kg body weight, to 5-wk-old male *ob/ob* mice weighing an average of ~30 g. After 8 wk on the analog **24**-treated chow, the mice gained 8–9 % less weight than control mice which were fed the same chow minus the compound (37.9 ± 0.9 vs. 41.4 ± 1.1 g/mouse, respectively) (Table 6). Food intake was slightly lower in the treated mice compared to controls (3.4 ± 0.54 vs. 3.6 ± 0.54 g/mouse per day.) Blood glucose was lower in the treated mice vs. controls (214 ± 16 vs 243.7 ± 27.6 mg/dl) (Table 6). The serum level of total cholesterol was lower in the treated mice compared to controls (220 ± 11 vs. 285 ± 8 mg/dl). There was a ~37% decrease in the level of LDL in the serum of treated mice compared to controls (50.2 ± 4.4 vs. 79.38 ± 2.85 mg/dl); however, no detectable change was observed in the HDL level in the serum of treated mice compared to controls (164.5 ± 5.3 vs. 164.83 ± 4.5 mg/dl) (Table 6). The triglyceride level in the liver tissues was significantly lower in the treated mice compared to controls, suggesting fatty liver conditions were ameliorated in the treated group (28 ± 1.0 vs. 42 ± 2.0 mg/g tissue). These results indicate that analog **24** is orally available in mice.

Overall, analog **24**, a methanesulfonamide derivative of fatostatin, exhibited the highest activity in a cell-based assay, and exhibited better *in vitro* and *in vivo* physicochemical properties than fatostatin or the other derivatives that were synthesized and evaluated. Analog **24** (FGH10019) is the most appropriate molecule for further testing in animal models, and this testing is currently under way.

Experimental Section

General

The general chemistry, experimental information, and syntheses of all other compounds are described in the Supporting Information. All tested compounds were >95% purity, as determined by examination of LC chromatogram (wavelength 235 nm) (Table S2) and/or combustion analysis (Table S3).

4-(2-Methoxyphenyl)-2-(2-propylpyridin-4-yl)thiazole (9)

A mixture of prothionamide (**3**) (700 mg, 3.88 mmol) and 2-bromo-1-(2-methoxyphenyl)ethanone (890 mg, 3.89 mmol) in ethanol (15 mL) was stirred for 0.5 h at 80°C, then cooled to 0°C. The yellow precipitate was filtered off and washed with cold ethanol. The residue was partitioned between EtOAc and saturated $NaHCO_3$ solution. The aqueous phase was extracted with EtOAc. The combined extracts were dried over Na_2SO_4 and concentrated to produce compound **9** (742 mg, 62%) as a yellow foam. ^{1}H NMR (300 MHz, $CDCl_3$): δ 8.60 (d, *J* = 5.2 Hz, 1H), 8.38 (d, *J* = 7.7 Hz, 1H), 8.06 (s, 1H), 7.78 (s, 1H), 7.71 (d, *J* = 5.2 Hz, 1H), 7.33 (t, *J* = 7.7 Hz, 1H), 7.09 (t, *J* = 7.7 Hz, 1H), 7.01 (d, *J* = 7.7 Hz, 1H), 3.95 (s, 3H), 2.87 (t, *J* = 7.7 Hz, 2H), 1.83 (m, 2H), 1.00 (t, *J* = 7.4 Hz, 3H); *m*/*z* = 311 $[M+H]^+$. Anal. ($C_{18}H_{18}N_2OS$) C, H, N, S.

N-Isopropyl-4-(2-(2-propylpyridin-4-yl)thiazol-4-yl)aniline (20)

Acetone (2.5 mL, 34.5 mmol) and acetic acid (2.0 mL, 34.5 mmol) were added to a stirred solution of compound **19** (1.02 g, 3.45 mmol) in CH_2Cl_2 (20 mL). After stirring for 1 h, $Na(AcO)_3BH$ (1.5 g, 6.9 mmol) was added, and the reaction mixture was stirred for 20 h. The reaction mixture was poured into saturated $NaHCO_3$ solution, and extracted with EtOAc. The combined extracts were dried over Na_2SO_4, and concentrated. Chromatography of the crude product was (SiO_2, 4:1 hexane: EtOAc) produced compound **20** (845 mg, 73%) as a white foam. ^{1}H NMR (300 MHz, $CDCl_3$): δ 8.61 (d, *J* = 5.2 Hz, 1H), 7.81 (d, *J* = 8.5 Hz, 2H), 7.76 (d, *J* = 1.4 Hz, 1H), 7.68 (dd, *J* = 1.4, 5.2 Hz, 1H), 7.34 (s, 1H), 6.65 (d, *J* = 8.5 Hz, 2H), 3.70 (m, 1H), 2.86 (t, *J* = 7.6 Hz, 2H), 1.83 (m, 2H), 1.25 (d, *J* = 6.0 Hz, 6H), 1.02 (t, *J* = 7.4 Hz, 3H); *m*/*z* = 338 $[M+H]^+$. Anal. ($C_{20}H_{23}N_3S$) C, H, N, S.

N-(4-(2-(2-Propylpyridin-4-yl)thiazol-4-yl)phenyl)methanesulfonamide (24)

Methanesulfonyl chloride (0.23 mL, 2.97 mmol) was added to a stirred solution of compound **19** (800 mg, 2.71 mmol) and pyridine (0.66 mL, 8.1 mmol) in CH_2Cl_2 (20 mL) at 0°C. After stirring for 0.5 h, the reaction mixture was poured into 2 M citric acid solution and extracted with EtOAc. The combined extracts were washed with saturated $NaHCO_3$ solution and brine, dried over Na_2SO_4, and concentrated to produce compound **24** (880 mg, 87%) as a yellow foam. ^{1}H NMR (300 MHz, CD_3OD): δ 8.55 (d, *J* = 5.2 Hz, 1H), 8.02 (d, *J* = 8.8 Hz, 2H), 7.95 (s, 1H), 7.90 (d, *J* = 1.9 Hz, 1H), 7.84 (dd, *J* = 1.9, 5.2 Hz, 1H), 7.34 (d, *J* = 8.8 Hz, 2H), 3.00 (s, 3H), 2.86 (t, *J* = 7.7 Hz, 2H), 1.80 (m, 2H), 1.01 (t, *J* = 7.3 Hz, 3H); *m*/*z* = 374 $[M+H]^+$. Anal. ($C_{18}H_{19}N_3O_2S_2$) C, H, N, S.

Supplementary Material

Refer to Web version on PubMed Central for supplementary material.

Acknowledgments

This work was supported in part by grants to M.U. from the Hoh-ansha Foundation and MEXT (Grant-in-Aid 21310140), and by grants to S.J.W. from the Hefni Technical Training Foundation and the National Institutes of Health (GM-63115). We also thank J. Sakai for an SREBP-2 antibody and a reporter gene construct, and T. Orihara, T. Morii, and T. Hasegawa for experimental support. S.K. is a postdoctoral fellow of JSPS. The Kyoto research group participates in the Global COE program “Integrated Materials Science” (#B-09).

Abbreviations

SREBP	sterol regulatory element-binding protein
S1P	site-1 protease
S2P	site-2 protease
SCAP	SREBP cleavage-activating protein
CHO-K1	Chinese hamster ovary- K1
PAMPA	parallel artificial membrane permeability assay
MVK	mevalonate kinase
HMGCR	HMG-CoA reductase
ACL	ATP citrate lyase
INSIG1	insulin-induced gene 1
MVD	mevalonate pyrophosphate decarboxylase
HMGCS1	HMG-CoA synthase 1
IDI1	isopentenyl-diphosphate delta isomerase 1
SCD1	stearoyl-CoA desaturase
LDLR	low-density lipoprotein receptor
RPL13A	ribosomal protein; L13a
B2M	Beta-2 microglobulin
GAPDH	glyceraldehyde-3-phosphate dehydrogenase
HDL	high-density lipoprotein
TG	triglycerides

References

1. Brown MS, Goldstein JL. The SREBP pathway: regulation of cholesterol metabolism by proteolysis of a membrane-bound transcription factor. Cell. 1997; 89:331–340. [PubMed: 9150132]
2. Osborne TF. Sterol regulatory element-binding proteins (SREBPs): key regulators of nutritional homeostasis and insulin action. J Biol Chem. 2000; 275:32379–32382. [PubMed: 10934219]
3. Sakai J, Duncan EA, Rawson RB, Hua X, Brown MS, Goldstein JL. Sterolregulated release of SREBP-2 from cell membranes requires two sequential cleavages, one within a transmembrane segment. Cell. 1996; 85:1037–1046. [PubMed: 8674110]
4. Goldstein JL, DeBose-Boyd RA, Brown MS. Protein sensors for membrane sterols. Cell. 2006; 124:35–46. [PubMed: 16413480]
5. Hua X, Nohturfft A, Goldstein JL, Brown MS. Sterol resistance in CHO cells traced to point mutation in SREBP cleavage-activating protein. Cell. 1996; 87:415–426. [PubMed: 8898195]

6. Radhakrishnan A, Sun LP, Kwon HJ, Brown MS, Goldstein JL. Direct binding of cholesterol to the purified membrane region of SCAP: mechanism for a sterol-sensing domain. Mol Cell. 2004; 15:259–268. [PubMed: 15260976]
7. Yang T, Espenshade PJ, Wright ME, Yabe D, Gong Y, Aebersold R, Goldstein JL, Brown MS. Crucial step in cholesterol homeostasis: sterols promote binding of SCAP to INSIG-1, a membrane protein that facilitates retention of SREBPs in ER. Cell. 2002; 110:489–500. [PubMed: 12202038]
8. Choi Y, Kawazoe Y, Murakami K, Misawa H, Uesugi M. Identification of bioactive molecules by adipogenesis profiling of organic compounds. J Biol Chem. 2003; 278:7320–7324. [PubMed: 12496288]
9. Kamisuki S, Mao Q, Abu-Elheiga L, Gu Z, Kugimiya A, Kwon Y, Shinohara T, Kawazoe Y, Sato S, Asakura K, Choo HY, Sakai J, Wakil SJ, Uesugi M. A small molecule that blocks fat synthesis by inhibiting the activation of SREBP. Chem Biol. 2009; 16:882–892. [PubMed: 19716478]
10. Comins DL, Mantlo NB. Regiospecific alpha-alkylation of 4-chloro(bromo) pyridine. J Org Chem. 1985; 50:4410–4411.
11. Bilgin AA. 2-Pyridylthiazoles II, synthesis and structure elucidations. Acta Pharm Turcica. 1988; 30:133–138.
12. Adams CM, Reitz J, De Brabander JK, Feramisco JD, Li L, Brown MS, Goldstein JL. Cholesterol and 25-hydroxycholesterol inhibit activation of SREBPs by different mechanisms, both involving SCAP and Insigs. J Biol Chem. 2004; 279:52772–52780. [PubMed: 15452130]
13. Horton JD, Shah NA, Warrington JA, Anderson NN, Park SW, Brown MS, Goldstein JL. Combined analysis of oligonucleotide microarray data from transgenic and knockout mice identifies direct SREBP target genes. Proc Natl Acad Sci U S A. 2003; 100:12027–12032. [PubMed: 14512514]
14. Lipinski CA, Lombardo F, Dominy BW, Feeney PJ. Experimental and computational approaches to estimate solubility and permeability in drug discovery and development settings. Adv Drug Deliv Rev. 1997; 23:3–25.

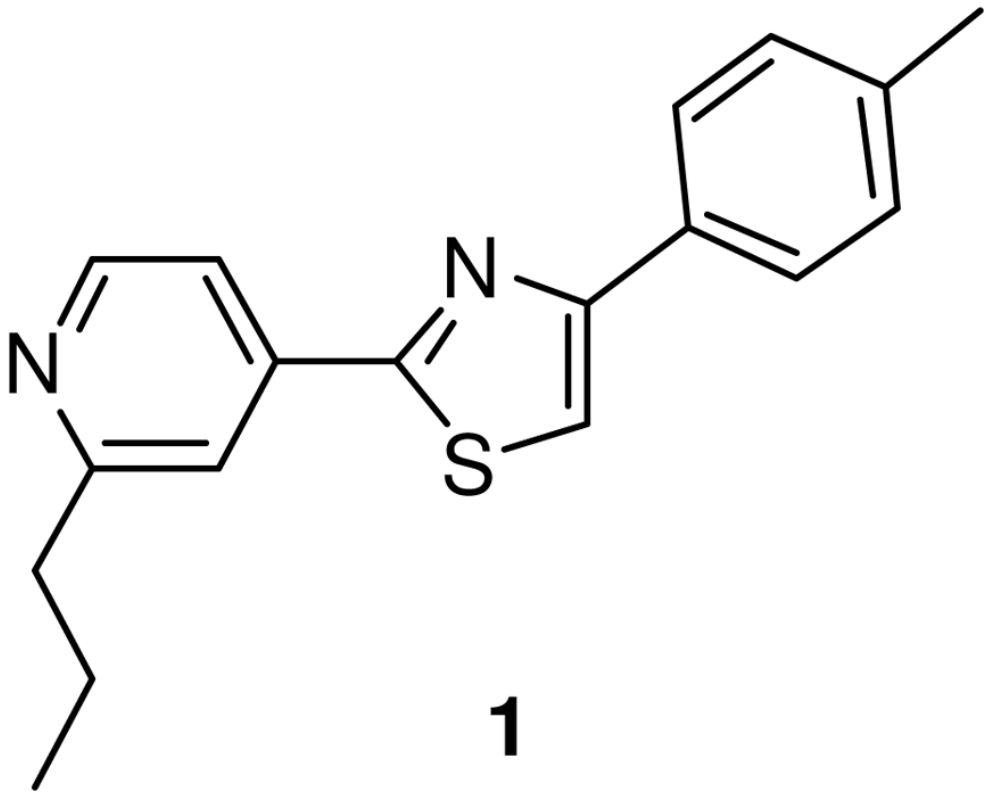

Figure 1.
Structure of fatostatin (**1**).

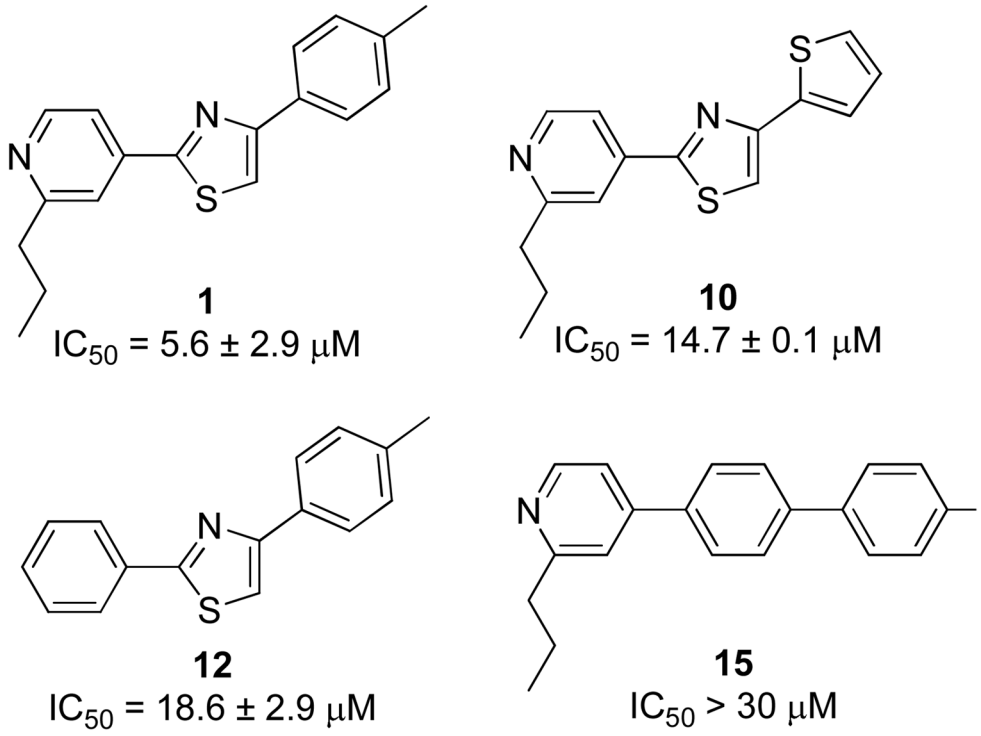

Figure 2.
Inhibitory activities of fatostatin (**1**) and analogs **10**, **12,** and **15** against the activation of SREBP in the luciferase reporter assay.

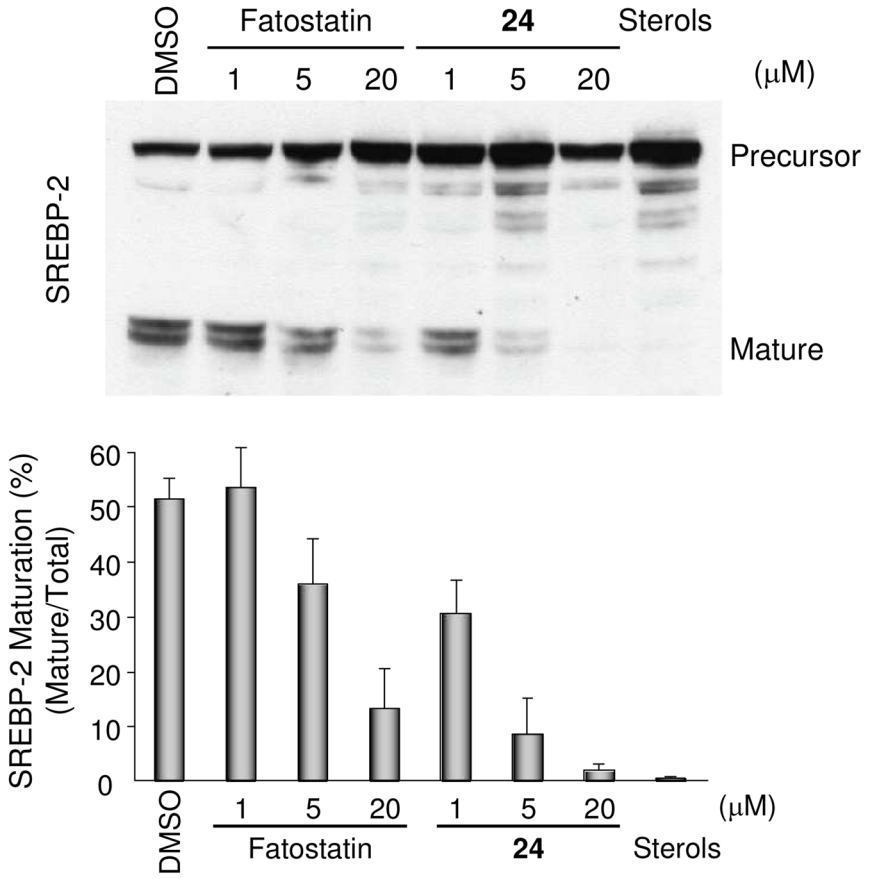

Figure 3.

Effects of fatostatin (**1**) and analog **24** on the proteolytic activation of SREBP-2 in cells. *Top*: western blot analysis of SREBP-2. CHO-K1 cells were treated with 1% (v/v) DMSO (vehicle), varied concentrations (1, 5, and 20 μM) of fatostatin (**1**) or compound **24**, or sterols (10 μg mL^{-1} cholesterol or 1 μg mL^{-1} 25- hydroxycholesterol). The precursor and mature forms of SREBP-2 were detected by an SREBP-2 antibody. The positions of the precursor and mature forms of SREBP- 2 are indicated. *Bottom*: quantification of the western blot analysis. Percentages of the mature form of SREBP-2 are shown. Values are means ± S.D. of three independent experiments.

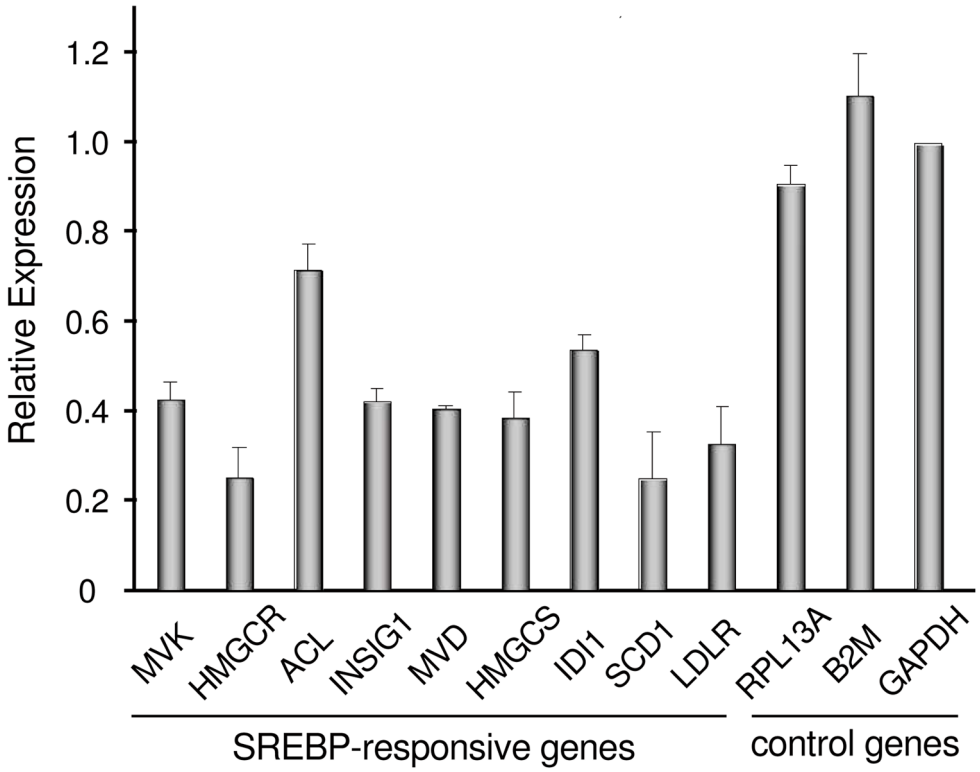

Figure 4.

Effects of analog **24** on the expression of SREBP-responsive genes in DU145 cells: mevalonate kinase, MVK; HMG-CoA reductase, HMGCR; ATP citrate lyase, ACL; insulin induced gene 1, INSIG1; mevalonate pyrophosphate decarboxylase, MVD; HMGCoA synthase 1, HMGCS; isopentenyl-diphosphate delta isomerase 1, IDI1; stearoyl-CoA desaturase, SCD1; LDL receptor, LDLR; ribosomal protein L13a, RPL13A; beta- 2 microglobulin, B2M; glyceraldehyde-3-phosphate dehydrogenase, GAPDH. Values are means ± SD of two independent experiments.

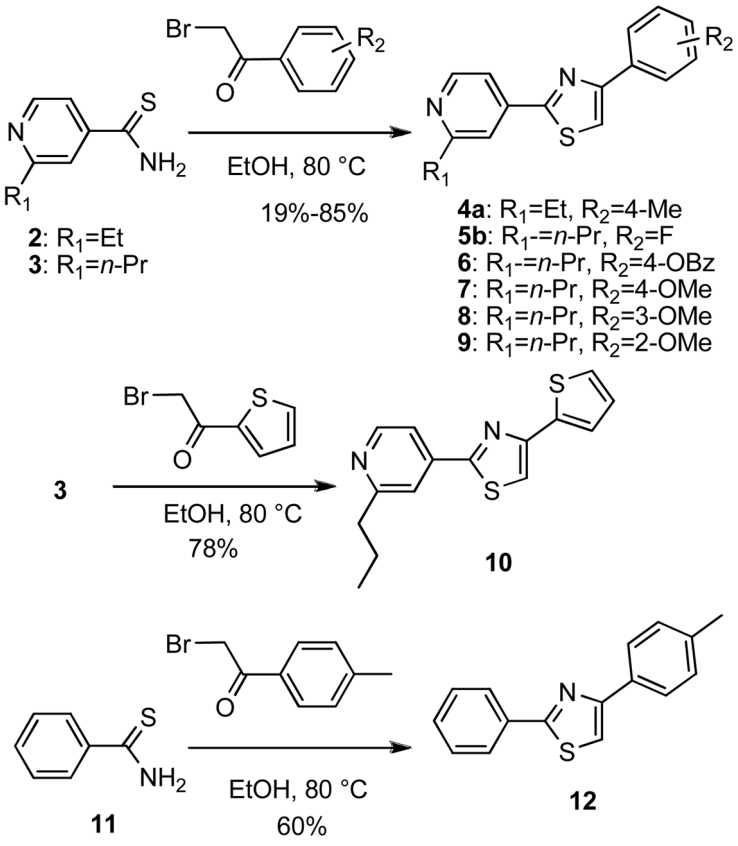

Scheme 1.
Synthesis of analogs **4**–**10**, **12**.

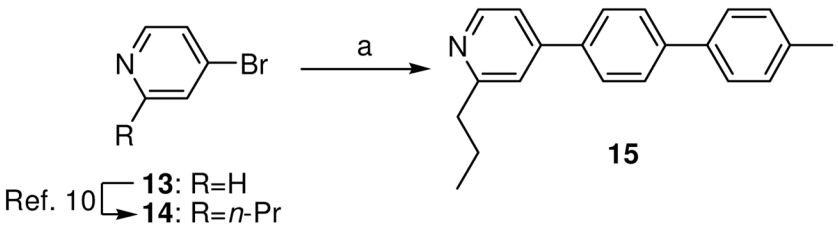

Scheme 2.

Synthesis of analog **15**.[a]

[a]Reagents and conditions: (a) 4′-methyl-4- biphenylboronic acid, $(Ph_3P)_4Pd$, K_2CO_3, DMF, H_2O, 80°C, 18 h, 52%

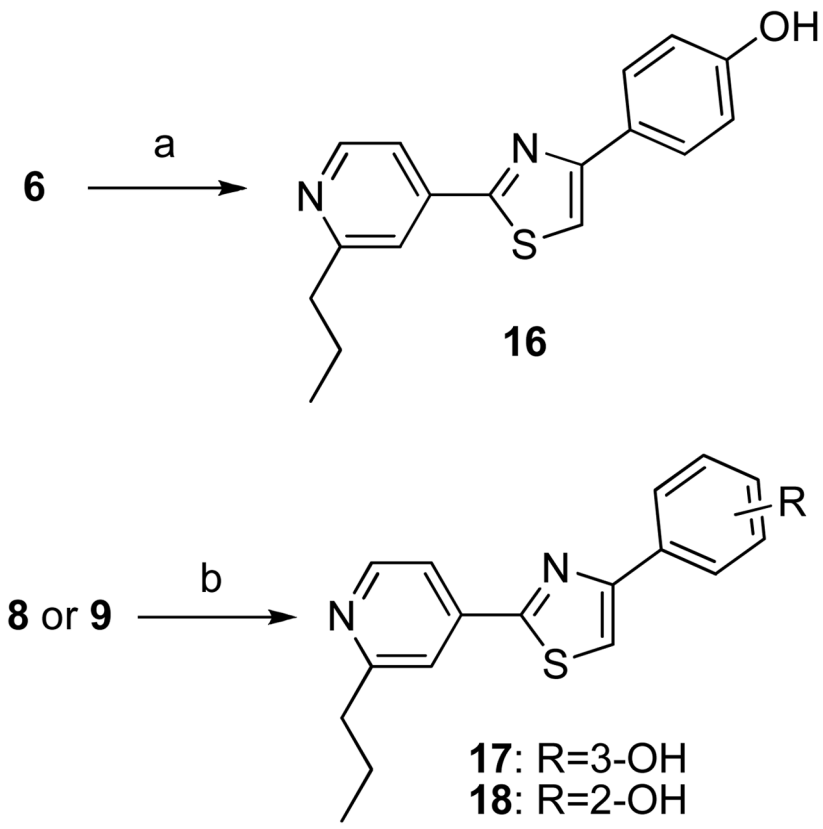

Scheme 3.
Synthesis of analogs **16**–**18**.[a]
[a]Reagents and conditions: (a) KOH aq. THF, MeOH, 60°C, 0.5 h, 80% (b) BBr_3, CH_2Cl_2, 0°C to room temperature, 6–14 h, 16–40%

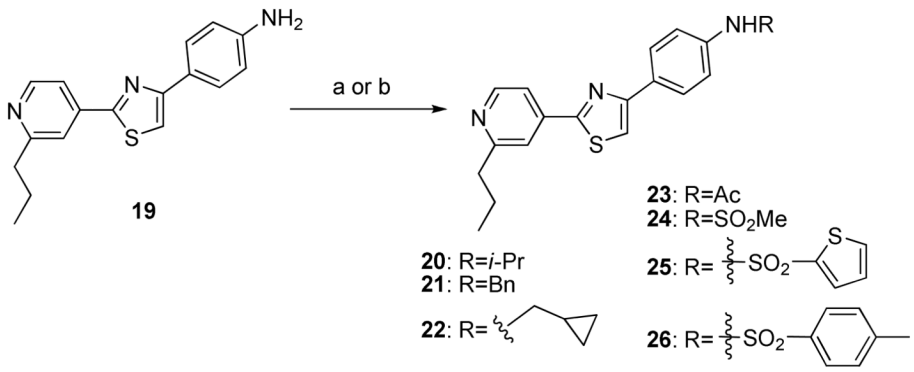

Scheme 4.

Synthesis of analogs **20**–**26**.[a]

[a]Reagents and conditions: (a) acetone, benzaldehyde or cyclopropanecarboxaldehyde, AcOH, $Na(AcO)_3BH$, CH_2Cl_2, room temperature, 19–21 h, 52–73% (b) acetyl chloride, methanesulfonyl chloride, thiophene sulfonylchloride or tosyl chloride, pyridine, CH_2Cl_2, 0°C to room temperature, 0.5–72 h, 14–87%

Table 1

Effects of pyridine group substitutions on the activation of SREBP.

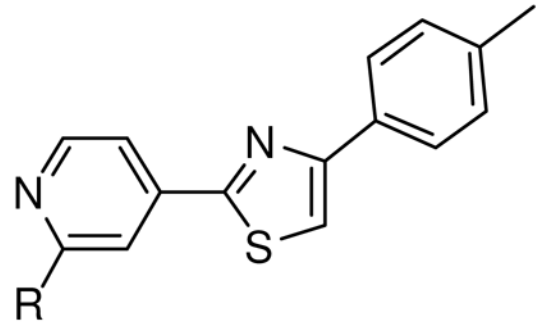

Compound	R	IC_{50} (μM)[a]
1	*n*-Pr	5.6 ± 2.9
4a	Et	6.8 ± 3.4
4b	H	>30

[a] All values are mean ± standard deviation, n ≥ 3.

Table 2

Effects of phenyl group substitutions on the activation of SREBP.

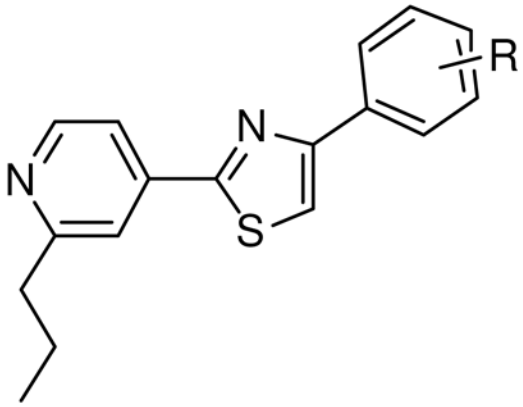

Compound	R	IC_{50} (μM)[a]
5a	H	23.0 ± 5.6
5b	4-F	12.4 ± 3.1
5c	4-Cl	10.7 ± 0.9
5d	4-Br	9.8 ± 0.6
6	4-OBz	7.7 ± 1.0
7	4-OMe	13.0 ± 3.3
8	3-OMe	10.2 ± 1.2
9	2-OMe	3.2 ± 0.4
16	4-OH	9.6 ± 1.2
17	3-OH	9.5 ± 0.4
18	2-OH	14.4 ± 0.2

[a] All values are mean ± standard deviation, n ≥ 3.

Table 3

Effects of *N*-substitution on the activation of SREBP.

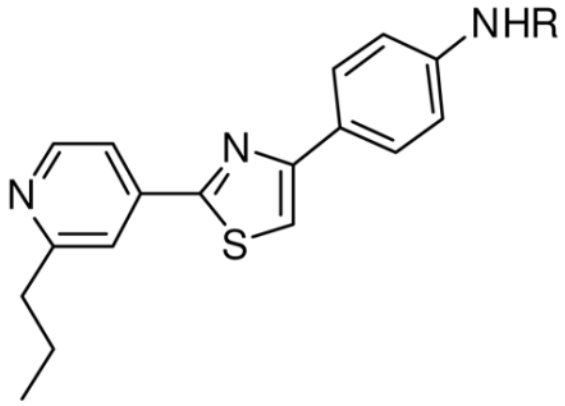

Compound	R	IC_{50} (μM)[a]
19	H	8.6 ± 2.0
20	Isopropyl	2.8 ± 0.4
21	Benzyl	3.0 ± 0.1
22	Methylcyclopropyl	4.9 ± 3.1
23	Acetyl	7.1 ± 1.5
24	Methansulfonyl	0.7 ± 0.2
25	Thiophenesulfonyl	0.9 ± 0.5
26	Tosyl	2.3 ± 0.0
27	*t*-Butoxycarbonyl	1.9 ± 0.2
25-hydroxy- cholesterol		0.3 ± 0.0

[a] All values are mean ± standard deviation, n ≥ 3.

Table 4

In vitro aqueous solubility at pH 3 and 7

Compound	Solubility pH 3 (μM)	Solubility pH 7 (μM)
1	80.0	2.0
20	>225	3.0
24	>225	33.0

Table 5

PAMPA permeability results for fatostatin (**1**) and analogs **20** and **24**

Compound	PAMPA Papp (10^{-6} cm/sec)	% Membrane retention	Reference ID	Reference PAMPA Papp (10^{-6} cm/sec)	Reference % membrane retention
1	0.7555	94	Warfarin	4.11	0
20	1.059	93.95	Warfarin	5.34	0
24	14.98	97.35	Warfarin	5.58	0

J Med Chem. Author manuscript; available in PMC 2012 July 14.

Table 6

Effect of feeding *ob/ob* mice analog **24**[a]

	Control	Treated
Body weight (g/mouse)	41.4 ± 1.1	37.9 ± 0.9*
Glucose (mg/dl)	243.7 ± 27.6	214 ± 16#
Cholesterol (dl)	285 ± 8	220 ± 11*
HDL (mg/dl)	164.83 ± 4.5	164.5 ± 5.3
LDL (mg/dl)	79.38 ± 2.85	50.2 ± 4.4*
TG in liver (mg/g tissue)	42 ± 2	28 ± 1*

[a]Male *ob/ob* mice were fed either normal chow (controls) or normal chow with compound analog **24** for 8 wk. Body weight and food intake was monitored and recorded daily. At the end of the experiments, serum constituents were determined and TG levels in liver were determined as we described previously.[9]

HDL: high-density lipoprotein; LDL: low-density lipoprotein; TG: triglycerides. Values are mean ± SE (n = 10):

*$P < 0.05$;

#$P = 0.09$.